MAXIMUM NORM ANALYSIS OF OVERLAPPING NON-MATCHING GRID DISCRETIZATIONS OF ELLIPTIC EQUATIONS*

XIAO-CHUAN CAI†, TAREK P. MATHEW,‡ AND MARCUS V. SARKIS§

Abstract. In this paper, we provide a maximum norm analysis of a finite difference scheme defined on overlapping non-matching grids for second order elliptic equations. We consider a domain which is the union of p *overlapping* subdomains where each subdomain has its own independently generated grid. The grid points on the subdomain boundaries need not match the grid points from adjacent subdomains. To obtain a global finite difference discretization of the elliptic problem, we employ standard stable finite difference discretizations within each of the overlapping subdomains and the different subproblems are coupled by enforcing *continuity* of the solutions across the boundary of each subdomain, by *interpolating* the discrete solution on adjacent subdomains. If the subdomain finite difference schemes satisfy a strong discrete maximum principle and if the overlap is sufficiently large, we show that the global discretization converges in optimal order corresponding to the largest truncation errors of the local interpolation maps and discretizations. Our discretization scheme and the corresponding theory allows any combination of lower order and higher order finite difference schemes in different subdomains. We describe also how the resulting linear system can be solved iteratively by a parallel Schwarz alternating method or a Schwarz preconditioned Krylov subspace iterative method. Several numerical results are included to support the theory.

Key words. Domain decomposition, overlapping non-matching grids, composite grids, finite difference discretizations, elliptic equations, schwarz alternating method, iterative methods

AMS(MOS) subject classifications. 65N20, 65F10

1. Introduction.

In recent years, much interest within the domain decomposition literature has focused on techniques for obtaining *global* discretizations of elliptic equations by combining discretizations on *local* non-overlapping or overlapping subdomains triangulated by *non-matching grids*. If each subdomain is independently triangulated using grids most suitable to its geometry or the local smoothness of the solution, then the resulting grids may not match at the boundaries. In the domain decomposition literature, techniques based on "Lagrange multipliers" and "mortar spaces" have been devised to "glue" together high accuracy local discretizations (for instance, based on spectral methods or p-version finite elements), see for instance, [2, 4, 5, 8, 9, 24], and also lower order local discretizations based on h-version finite elements, see for instance, [1, 7, 21, 33]. By contrast, in the finite difference literature, even prior to the development of domain decomposition techniques, several early works have focused on discretizations on *non-matching* composite grids, see [11, 17, 19, 29, 30]. Even though the available theory is limited, several large computations have shown that non-matching grid techniques have tremendous advantages over the traditional matching grid meth-

* The work was supported in part by the NSF grants ASC-9457534, ECS-9527169, and ECS-9725504.

† Department of Computer Science, University of Colorado, Boulder, CO 80309-0430. *cai@cs.colorado.edu*

‡ Department of Mathematics, University of Wyoming, Laramie, WY 82071-3036. *mathew@uwyo.edu*

§ Mathematical Sciences Department, Worcester Polytechnic Institute, Worcester, MA 01609-2280. *msarkis@wpi.edu*

ods due to the time saved on the grid generation stage of the computation, especially for problems with complex geometry ([20, 30]).

In [29], Starius provided an analysis for the two subdomain case, and our purpose in this paper is to extend the result of Starius on the maximum norm stability of global finite difference discretizations of elliptic equations, to the case of many subdomains. The extension we consider will be applicable to domains with general shapes, involve an arbitrary number of composite subgrids, and allow local finite difference schemes of any order, provided the discretizations satisfy locally a maximum principle and the overlap between the subdomains is sufficiently large. Further, the analysis, based on constructing a *contraction mapping*, will permit *parallel* solution of the subgrid problems iteratively.

The linear elliptic equation we consider will be of the following form on a domain Ω in R^2 or R^3:

$$\left\{ \begin{array}{rcll} Lu \equiv -\Delta u + \vec{b}(x) \cdot \nabla u + c(x)u & = & f(x) & \text{in } \Omega \\ u & = & g(x) & \text{on } \partial\Omega. \end{array} \right. \tag{1}$$

Throughout the rest of this paper, we will assume that $c(x) \geq c_0 > 0$ on Ω, and that the forcing term f, the boundary value function g, the coefficients $\vec{b}$ and c, and the exact solution u are *smooth.* On each subdomain, we will consider local discretizations that satisfy a *discrete maximum principle.*

One of the fundamental issues in studying non-matching grid methods is to understand the relation between the order of the global discretization error, the orders of the subdomain discretization errors, the orders of the interpolation errors between non-matching subgrids, and the size of the overlap. Suppose that Ω is the union of p overlapping subdomains $\Omega_1', \ldots, \Omega_p'$. Let h_i be the mesh size of subdomain Ω_i', and let p_i and q_i be the orders of the discretization and interpolation errors on Ω_i' and $\partial\Omega_i'$, respectively. Further, let $\Omega_{\Gamma_i^c}$ denote a neighborhood of the subdomain boundary segment $\Gamma_i^c = \partial\Omega_i' \cap \Omega$ containing all grid points used in the local interpolation. Then we show in this paper that the maximum norm of the global error is bounded by

$$C\left(1 + \frac{\sigma}{1-\delta_0}\right)\left(\sum_{i=1}^{p} h_i^{p_i} \|u\|_{p_i+2,\infty,\Omega_i'} + \sum_{i=1}^{p} h_i^{q_i} \|u\|_{q_i,\infty,\Omega_{\Gamma_i^c}}\right), \tag{2}$$

which yields a bound that depends on the local smoothness of the solution (so that for instance, the mesh size h_i may need to be chosen smaller on a subregion Ω_i' where $\|u\|_{p_i+2,\infty,\Omega_i'}$ or $\|u\|_{q_i,\infty,\Omega_{\Gamma_i^c}}$ is large). Here σ is a bound for the maximum norm of the subdomain interpolation operators. $\delta_0 < 1$ is a parameter that depends on σ and on a contraction factor ρ associated with homogeneous solutions of subdomain elliptic equations. For elliptic equations with $c(x) \geq c_0 > 0$, it is known that the maximum norm of a homogeneous solution in the true interior of a domain is bounded by the maximum norm of its boundary data multiplied by a factor $0 < \rho < 1$, see for instance Smoller [28] or Lions [23]. For the discrete case, see [16, 26]. The parameter δ_0 is the product of σ with the largest factor ρ from different subdomains. Thus, factor δ_0 may

depend on the size of the overlap between the subdomains, while σ may depend on the choice of the local grids.

The method and the theory described in this paper are quite different from the mortar based approach developed in [7]. In the mortar method, the discretization error is proved to be totally independent of the overlap size. Whereas the method to be studied in this paper has some degree of dependency on the overlap size but is a lot easier to implement than any of the mortar type methods. The mortar theory of [7] is valid only for the two-subdomain case involving simple interfaces without corner points, while the maximum principle based theory developed in this paper applies for any number of subdomains in both R^2 and R^3.

Although the focus of this paper is on the accuracy of the overlapping non-matching grid method, we will include a short discussion on Schwarz type iterative methods for solving the resulting linear system of equations. We prove that if the overlap is sufficiently large, the convergence of the Schwarz method is independent of the mesh sizes. Related topics can also be found in the book [27].

The rest of the paper is organized as follows. In Section 2, we describe a finite difference procedure for obtaining a global discretization on non-matching composite grids, see [11, 29]. In Section 3, we describe a technique for analyzing the stability of the global discretization. In Section 4, we apply the stability result of Section 3 to derive bounds for the accuracy of the global discrete solution. In Section 5, we describe two iterative procedures for solving the resulting linear system satisfied by the global discrete solution, by using a parallel Schwarz alternating method and an additive Schwarz preconditioned Krylov subspace iterative method. Finally, in Section 6, we present the results of sample numerical tests.

2. Discretization on overlapping non-matching grids. The global discretization method we use is the composite grid method, see for instance, Starius [29] and Cheshire and Henshaw [11]. It involves independently discretizing the elliptic equation $Lu = f$ on each of the subgrids and coupling the discretizations by requiring *continuity* of the solutions across the boundaries.

Given a domain Ω, we first choose a partition of Ω into p *non-overlapping* subdomains such that

$$\overline{\Omega} = \cup_{i=1}^{p} \overline{\Omega}_i, \quad \Omega_i \cap \Omega_j = \emptyset, \quad \text{for} \quad j \neq i.$$

We then enlarge each subdomain Ω_i to include all points in Ω within a distance $\theta > 0$ and denote the resulting enlarged subdomain by $\Omega_i^{'}$

$$\Omega_i^{'} \equiv \{x \in \Omega : dist\,(x, \Omega_i) \leq \theta\}\,.$$

Thus the enlarged domains will satisfy

$$\Omega \subset \left(\Omega_1^{'} \cup \cdots \cup \Omega_p^{'}\right).$$

On each subdomain $\Omega_i^{'}$ we independently construct a grid of size h_i. We will use $\Omega_{i,h_i}^{'}$ to denote the grid on $\Omega_i^{'}$, for $i = 1, \ldots, p$. The grid points on the boundary $\partial\Omega_i^{'}$ need not align with the grid points in the adjacent subdomains, see Fig 1.

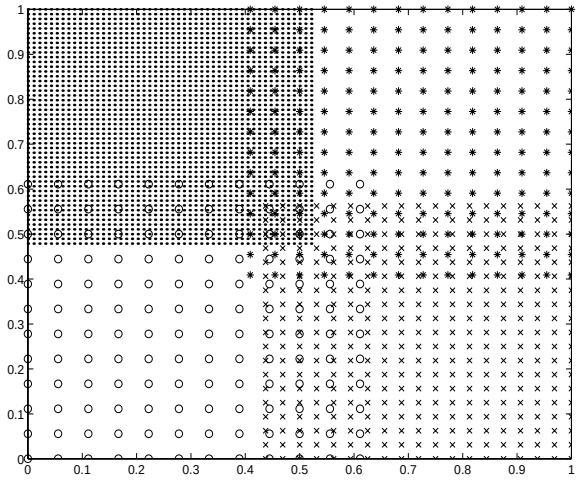

FIG. 1. *An example of a global grid consisting of four overlapping non-matching subgrids.*

On grid $\Omega_{i,h_i}^{'}$, we use U_{h_i} to denote the discrete solution approximating the exact solution u on $\Omega_{i,h_i}^{'}$. The global solution U_h is then denoted as the collection of local solutions

$$U_h = \left(U_{h_1}, \ldots, U_{h_p}\right).$$

We use the notation Γ_i to denote the portion of the boundary $\partial\Omega_i^{'}$ intersecting $\partial\Omega$, i.e., $\Gamma_i \equiv \partial\Omega_i^{'} \cap \partial\Omega$. We can then partition $\partial\Omega_i^{'}$ into two pieces, Γ_i and its complement $\Gamma_i^c \equiv \partial\Omega_i^{'} \setminus \Gamma_i$:

$$\partial\Omega_i^{'} = \left(\partial\Omega_i^{'} \cap \partial\Omega\right) \cup \left(\partial\Omega_i^{'} \cap \Omega\right) = \Gamma_i \cup \Gamma_i^c.$$

We use Γ_{i,h_i} to denote the grid on Γ_i and Γ_{i,h_i}^c the grid on Γ_i^c.

To motivate the composite grid discretization, we observe that the solution $u(x)$ of the elliptic equation (1) satisfies:

$$\left\{\begin{array}{rcll} Lu_i & = & f_i, & \text{on } \Omega_i^{'} \\ u_i & = & g_i, & \text{on } \Gamma_i \\ u_i & = & u & \text{on } \Gamma_i^c, \end{array}\right.$$

where u_i denotes the continuous restriction of u to $\Omega_i^{'}$, where f_i is the restriction of f to $\Omega_i^{'}$, and g_i is the restriction of g to Γ_i.

Analogous to the continuous case above, the local discretization on $\Omega_{i,h_i}^{'}$ of problem (1) in the composite grid method will approximate the above problem:

$$\left\{\begin{array}{rcll} L_{h_i}U_{h_i} & = & f_{h_i}, & \text{on } \Omega_{i,h_i}^{'} \\ U_{h_i} & = & g_{h_i}, & \text{on } \Gamma_{i,h_i} \\ U_{h_i} & = & I^i U_h & \text{on } \Gamma_{i,h_i}^c, \end{array}\right. \tag{3}$$

where f_{h_i} is the restriction of the forcing term f to the grid points in Ω_{i,h_i}, where g_{h_i} is the restriction of the Dirichlet boundary data g to the grid points in Γ_{i,h_i} and $I^i U_h$ will be suitably chosen as an *interpolation* of the discrete solution U_h to enforce *continuity* of the local solution. If a grid point in $\partial\Omega'_{i,h_i}$ matches with a grid point in an adjacent grid Ω'_{j,h_j} then $I^i U_h$ would ideally be chosen to equal the grid value of U_{h_j} at that grid point. However, for non-matching grids, we define $I^i U_h$ as an *interpolation* of the grid values of U_{h_j} on adjacent grid points.

Assumption $A1$ (**Truncation error of local discretizations**): *We assume that the local discretizations have a truncation error $\alpha_i(x)$ of order p_i at a point x in Ω'_{i,h_i}.*

More specifically, if $u(x)$ is a smooth function, and u_{h_i} denotes the restriction of $u(x)$ to the grid points in Ω'_{i,h_i}, then we define the local truncation error $\alpha_i(x)$ at grid point x by

$$(L_{h_i} u_{h_i})(x) = (Lu)(x) + \alpha_i(x). \tag{4}$$

We assume that the local discretization scheme is chosen so that the truncation error $\alpha_i(x)$ satisfies the following bounds

$$|\alpha_i(x)| \leq C h_i^{p_i} \|u\|_{p_i+2,\infty,\Omega'_i}.$$

Here $\|u\|_{p_i+2,\infty,\Omega'_i}$ denotes the Sobolev $W^{p_i+2,\infty}(\Omega'_i)$ norm of u (Grisvard [18]).

We require intergrid interpolation maps I^i for $i = 1, \cdots, p$, to define the boundary data $I^i U_h$ in the global discretization (7), where $I^i U_h$ uses the value of U_{h_j} at grid points in the adjacent domains Ω'_{j,h_j} for $j \neq i$. This interpolation map I^i is a *linear transformation*

$$I^i : U_h \rightarrow U_{h_i,\Gamma^c_{i,h_i}}.$$

Assumptions $A2$ (**Subgrid interpolation**): *We assume that the interpolation map I^i does not use values of U_{h_i} in Ω'_{i,h_i}, and further, that I^i only uses nodal values at grid points x in $\cup_{j\neq i}\overline{\Omega}_{j,h_j}$, i.e., I^i does not use nodal values at grid points in the domains $\{\Omega'_{j,h_j} \setminus \overline{\Omega}_{j,h_j}\}_{j\neq i}$.*

As an example, consider Fig 2. Let $\times$ denote a grid point in $\partial\Omega'_{i,h_i}$ and let $\circ$ denote grid points in Ω'_{j,h_j} for some $j \neq i$. If $\times$ lies in the *convex hull* of the grid points $\circ$, then the interpolated value at $\times$ can be obtained by linear interpolation of the nodal values on the triangle with vertices $\circ$. We need to define a similar interpolation rule for each grid point on Γ^c_{i,h_i}. For a suitable ordering of the grid points in $\cup_{j=1}^{p}\overline{\Omega}'_{j,h_j}$ and in $\partial\Omega'_{i,h_i}$ the stencil is stored in the matrix I^i.

REMARK 2.1. *The intergrid interpolation maps I^i may also be defined by matching various moments of the traces of the subdomain functions on the interfaces, as in mortar methods [7].*

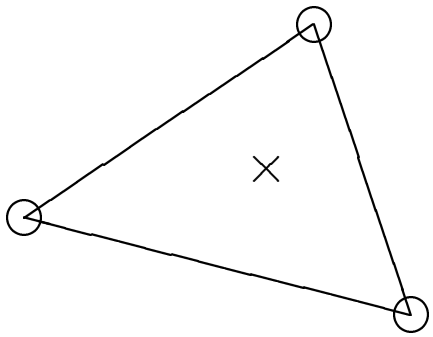

FIG. 2. *Example of an interpolation stencil*

The *maximum norm* of each interpolation map I^i is denoted by $\|I^i\|_{\infty,\Gamma^c_{i,h_i}}$. It corresponds to the largest absolute row sum of the matrix I^i. We use σ to denote the largest of the maximum norms amongst all the interpolation maps

$$\sigma \equiv \max_i \|I^i\|_{\infty,\Gamma^c_{i,h_i}}. \tag{5}$$

For example, if $I^i U_h$ are all obtained at each grid point by piecewise linear interpolation of nodal values of U_h on adjacent domains, then the linear interpolation stencil will correspond to a *convex* combination of three nodal values of U_h in adjacent domains. For such a stencil, we obtain

$$\|I^i\|_{\infty,\Gamma^c_{i,h_i}} = 1, \qquad \text{for } i = 1, \cdots, p,$$

and consequently $\sigma = 1$.

Assumption *A*3 (**Interpolation error**): *The error $I - I^i$ of the interpolation operator I^i is of order q_i.*

Let $u(x)$ be a smooth function. Then the *interpolation error* $\beta_i(x)$ at a grid point $x \in \partial\Omega'_{i,h_i}$ is defined as:

$$\beta_i(x) \equiv u(x) - \left(I^i u\right)(x).$$

This interpolation error $\beta_i(x)$ can be estimated using a Taylor series expansion of $u(x)$ involving adjacent grid points in an enlarged region $\Omega_{\Gamma^c_i}$ containing Γ^c_{i,h_i}. We assume that the interpolation map I^i is chosen such that the following bound holds for the interpolation error $\beta_i(x)$ at the point x

$$|\beta_i(x)| = |\left(I - I^i\right) u| \leq C h_i^{q_i} \|u\|_{q_i,\infty,\Omega_{\Gamma^c_i}}, \tag{6}$$

where $\|\cdot\|_{q_i,\infty,\Omega_{\Gamma^c_i}}$ denotes the Sobolev $W^{q_i,\infty}(\Omega_{\Gamma^c_i})$ norm and C is a constant independent of h_i.

The *global discretization* for $U_h = (U_{h_1}, \cdots, U_{h_p})$ in the composite grid method is obtained by *coupling* the local discretizations by requiring that the solution "matches" the interpolation of the discrete solution from adjacent grids on Γ^c_{i,h_i}

$$\left\{ \begin{array}{rcll} L_{h_i} U_{h_i} & = & f_{h_i}, & \text{on } \Omega'_{i,h_i} \\ U_{h_i} & = & g_{h_i}, & \text{on } \Gamma_{i,h_i} \\ U_{h_i} & = & I^i U_h, & \text{on } \Gamma^c_{i,h_i}, \end{array} \right. \tag{7}$$

for $i = 1, \cdots, p$. The above linear system can be solved iteratively, for instance, by using the Schwarz alternating procedure, see Section 5.

For example, in the case of two composite grids, our global discrete solution is denoted by $U_h = (U_{h_1}, U_{h_2})$, and it satisfies

$$\left\{ \begin{array}{rcll} L_{h_1} U_{h_1} & = & f_{h_1}, & \text{on } \Omega'_{1,h_1} \\ U_{h_1} & = & g_{h_1}, & \text{on } \Gamma_{1,h_1} \\ U_{h_1} & = & I^1 \left(U_{h_1}, U_{h_2} \right), & \text{on } \Gamma^c_{1,h_1}, \end{array} \right.$$

and

$$\left\{ \begin{array}{rcll} L_{h_2} U_{h_2} & = & f_{h_2}, & \text{on } \Omega'_{2,h_2} \\ U_{h_2} & = & g_{h_2}, & \text{on } \Gamma_{2,h_2} \\ U_{h_2} & = & I^2 \left(U_{h_1}, U_{h_2} \right), & \text{on } \Gamma^c_{2,h_2}. \end{array} \right.$$

If there are n_1 grid points in $\overline{\Omega}'_{1,h_1}$ and n_2 grid points in $\overline{\Omega}'_{2,h_2}$ (including all the grid points on the boundaries), then the above global discretization yields a system of $n_1 + n_2$ linear algebraic equations for the discrete solution $U_h = (U_{h_1}, U_{h_2})$, including the boundary conditions on $\partial\Omega$.

REMARK 2.2. *Due to the non-symmetric nature of the interpolation maps, the above global discretization does not yield a symmetric linear system in general, even if the local discretizations are symmetric.*

REMARK 2.3. *If the subgrids match, then the global discretization just introduced reduces to the usual discretization on the whole domain. The global linear system can also be reduced by removing the redundant variables.*

3. Maximum norm stability of the global discretization. In this section, we prove that the global discretization (7) is solvable, and further that it is stable in the maximum norm. We first state the assumptions under which this analysis is valid.

Assumption B1 (**Local stability**): *We assume that the local finite difference discretizations (3) are chosen so that they are stable in the maximum norm.*

More precisely, for $i = 1, \cdots, p$, we assume that there exists a constant K_i independent of h_i such that if U_{h_i} solves

$$\left\{ \begin{array}{rcll} L_{h_i} U_{h_i} & = & f_{h_i}, & \text{in } \Omega'_{i,h_i} \\ U_{h_i} & = & g_{h_i}, & \text{on } \Gamma_{i,h_i}, \\ U_{h_i} & = & z_{h_i}, & \text{on } \Gamma^c_{i,h_i}, \end{array} \right.$$

then for $i = 1, \cdots, p$

$$\|U_{h_i}\|_{\infty,\Omega_i'} \leq K_i \|f_{h_i}\|_{\infty,\Omega'_{i,h_i}} + \max\{\|g_{h_i}\|_{\infty,\Gamma_{i,h_i}}, \|z_{h_i}\|_{\infty,\Gamma^c_{i,h_i}}\}.$$

We note that in the special case that $f_{h_i} = 0$, then the above stability assumption requires that a *homogeneous* solution U_{h_i} satisfies a *weak* discrete maximum principle

$$\|U_{h_i}\|_{\infty,\Omega_i'} \leq \max\{\|g_{h_i}\|_{\infty,\Gamma_{i,h_i}}, \|z_{h_i}\|_{\infty,\Gamma^c_{i,h_i}}\}.$$

Assumption B2 (**Contraction factor for homogeneous solutions**): *We assume that the local discretizations satisfy a strong discrete maximum principle of the following form. If e_{h_i} is the solution of the following homogeneous problem on the overlapping domain $\Omega_i^{'}$*

$$\left\{ \begin{array}{rcll} L_{h_i} e_{h_i} & = & 0, & on\ \Omega'_{i,h_i} \\ e_{h_i} & = & 0, & on\ \Gamma_{i,h_i}, \\ e_{h_i} & = & z_{h_i}, & on\ \Gamma^c_{i,h_i}, \end{array} \right.$$

then in the non-overlapping domain Ω_i

$$\|e_{h_i}\|_{\infty,\overline{\Omega}_i} \leq \rho_{i,h_i} \|z_{h_i}\|_{\infty,\Gamma^c_{i,h_i}}, \tag{8}$$

where $0 < \rho_{i,h_i} < 1$ is a contraction factor for the error on the i'th grid. It will further be assumed that

$$\rho_{i,h_i} \leq \rho_i < 1,$$

for some $\rho_i < 1$ when h_i is sufficiently small.

Below, we briefly discuss some results concerning assumption $B2$. Given an elliptic operator $Lu \equiv -\Delta u + \vec{b}(x) \cdot \nabla u + c(x)u$, its contraction factor ρ_i on subdomain Ω_i' can be defined in the continuous case as

$$\rho_i \equiv \max_{\overline{\Omega}_i} w_i(x), \quad \text{where} \quad \left\{ \begin{array}{rcll} Lw_i & = & 0, & \text{in } \Omega_i' \\ w_i & = & 0, & \text{on } \Gamma_i \\ w_i & = & 1, & \text{on } \Gamma_i^c. \end{array} \right.$$

For the continuous problem, ρ_i may depend on the magnitudes of $\vec{b}(x)$, c_0 (where $c(x) \geq c_0 > 0$), the overlap parameter θ, and the shape and diameter of Ω_i'. When $c(x) \geq c_0 > 0$, the contraction factor ρ_i can be estimated for the continuous problem by constructing "barrier" (or "comparison") functions $B_i(x) \geq w_i(x) \geq 0$ satisfying

$$\left\{ \begin{array}{rcll} LB_i & \geq & 0, & \text{in } \Omega_i' \\ B_i & \geq & 0, & \text{on } \Gamma_i \\ B_i & \geq & 1, & \text{on } \Gamma_i^c \end{array} \right. \quad \Longrightarrow \quad \rho_i = \max_{\overline{\Omega}_i} w_i(x) \leq \max_{\overline{\Omega}_i} B_i(x),$$

see for instance [23, 25]. In particular, a barrier function $B_i(x)$ satisfying $LB_i \geq c_0/2 > 0$ and

$$\max_{\overline{\Omega}_i} B_i(x) \leq e^{-\alpha\theta} \quad \Longrightarrow \quad \rho_i \leq e^{-\alpha\theta},$$

can be constructed for the continuous problem [23, 25, 28]. Here $\alpha > 0$ depends on c_0 (indeed, $\alpha \to 0$ as $c_0 \to 0$) but is independent of the overlapping parameter θ. When $c(x) = 0$, two cases may be distinguished:
Case 1. $c(x) = 0$ and Ω_i' is a "floating" subdomain (i.e., $\overline{\Omega}_i' \subset \Omega$). In this case, $\rho_i = 1$ for Ω_i' (since constants will be homogeneous solutions).
Case 2. $c(x) = 0$ and the boundary $\partial\Omega_i'$ intersects the zero Dirichlet boundary $\partial\Omega$ on a set of positive measure

$$meas\,(\partial\Omega_i' \cap \partial\Omega) > 0.$$

In this case, we may have a contraction factor $\rho_i < 1$ for Ω_i', due to the influence of the zero Dirichlet boundary conditions (see Remark 4.4). Rigorous results for this case however are not known to the authors (the procedure in [23, 25] for constructing barrier functions fails in this case).

Next, we briefly discuss assumption $B2$ for finite difference discretizations satisfying a discrete maximum principle. A contraction factor ρ_{i,h_i} can be defined analogous to the continuous case. Furthermore, this discrete contraction factor can be estimated if discrete barrier functions are constructible. Below, we indicate the key idea in [26] that can be used to relate the discrete contraction factor ρ_{i,h_i} to the continuous contraction factor ρ_i when h_i is *sufficiently small*, when $c_0 > 0$ and when a discrete maximum principle holds within each subdomain Ω_{i,h_i}'. Let $B_i(x)$ be the continuous barrier function defined on Ω_i' satisfying

$$\left\{ \begin{array}{rcll} LB_i & \geq & \dfrac{c_0}{2}, & \text{in } \Omega_i' \\ B_i & \geq & 0, & \text{on } \Gamma_i \\ B_i & \geq & 1, & \text{on } \Gamma_i^c \end{array} \right.$$

as constructed in [23, 25]. Using $B_i(\cdot)$ define a *discrete* barrier function B_{h_i} by restricting $B_i(\cdot)$ to the local gridpoints $x_j \in \Omega_{i,h_i}'$. Let the local discretization be accurate to order p_i (where $p_i \geq 1$) with truncation error $t_j h_i^{p_i}$ at a grid point $x_j \in \Omega_{i,h_i}'$. Then, the following will hold

$$\begin{array}{rcl} L_{h_i} B_{h_i}(x_j) & = & LB_i(x_j) + t_j h_i^{p_i} \\ & \geq & \dfrac{c_0}{2} + t_j h_i^{p_i} \geq 0. \end{array}$$

The last inequality above will hold only if h_i is sufficiently small such that

$$h_i^{p_i} \leq \frac{c_0}{2|t_j|}, \quad \forall x_j \in \Omega_{i,h_i}',$$

see [26] (the term t_j will generally depend on higher order derivatives of $B_i(x)$ evaluated at points $\tilde{x}_j$ near x_j). Since the discrete barrier function equals the continuous barrier

function at the grid points in Ω'_{i,h_i} (by construction), it immediately follows that for the above h_i

$$\rho_{i,h_i} \leq \rho_i.$$

Throughout the rest of this paper, we will use ρ_i (omiting ρ_{i,h_i}) to denote the discrete contraction factor (though according to the above discussion, it will be bounded by the continuous contraction factor for small h_i). Other discussions of discrete contraction factors may be found in [12, 16].

It can also be noted that the local contraction factors ρ_i will generally deteriorate ($\rho_i \to 1$) if $diam\,(\Omega'_i) \to 0$. (A quantitative estimate of the contraction factor's dependence on the diameter of the domain can be obtained by mapping a domain Ω'_i to a reference domain of diameter 1, and studying the change in the coefficient c_0).

Assumption B3 (**Product of σ and ρ_i**): *Recall that ρ_i denotes the maximum norm contraction factor for each subdomain as in (8), and σ denotes the largest maximum norm of the interpolation maps, as in (5). We assume that*

$$\max_i \ (\rho_i \sigma) = \delta_0 < 1.$$

We now describe the stability result for the global discretization.

LEMMA 3.1. *Let $W_h = \left(W_{h_1}, \cdots, W_{h_p}\right)$ satisfy the following discrete equations*

$$\left\{ \begin{array}{rcll} L_{h_i} W_{h_i} & = & f_{h_i}, & on\ \Omega'_{i,h_i} \\ W_{h_i} & = & g_{h_i}, & on\ \Gamma_{i,h_i} \\ W_{h_i} - I^i W_h & = & z_{h_i}, & on\ \Gamma^c_{i,h_i}. \end{array} \right. \tag{9}$$

If assumptions A1, A2, A3, B1, B2 and B3 hold, then

$$\sum_{i=1}^{p} \|W_{h_i}\|_{\infty,\Omega'_{i,h_i}} \leq \left(1 + \frac{\sigma}{1-\delta_0}\right) \left(\sum_{i=1}^{p} K_i \|f_{h_i}\|_{\infty,\Omega'_{i,h_i}} + \sum_{i=1}^{p} \max\{\|g_{h_i}\|_{\infty,\Gamma_{i,h_i}}, \|z_{h_i}\|_{\infty,\Gamma^c_{i,h_i}}\} \right),$$

where K_i, σ and δ_0 are independent of h_i.

Proof. We apply Picard's theorem on the existence of a fixed point for contraction mappings as follows, see for instance [3]. Let $\mathcal{H}$ be a complete metric space endowed with a metric $d\,(\cdot,\cdot)$, and let $\mathcal{T} : \mathcal{H} \to \mathcal{H}$ be a contraction mapping satisfying

$$d\,(\mathcal{T}U, \mathcal{T}V) \leq \delta_0 d\,(U, V)\,,$$

for all U and V in $\mathcal{H}$, where $0 < \delta_0 < 1$. Then, $\mathcal{T}$ has a unique fixed point $U^* \in \mathcal{H}$ satisfying

$$\mathcal{T}U^* = U^*,$$

and given any initial iterate $U^0 \in \mathcal{H}$ we have the estimate

$$d\left(U^0, U^*\right) \leq \frac{d\left(U^0, \mathcal{T}U^0\right)}{1-\delta_0}.$$

In order to apply Picard's contraction mapping principle, we define $\mathcal{H}$, a metric $d(\cdot,\cdot)$ and a contraction mapping $\mathcal{T} : \mathcal{H} \to \mathcal{H}$ such that the solution of the discrete problem (9) is the fixed point of $\mathcal{T}$. Accordingly, we define $\mathcal{H}$ as follows

$$\mathcal{H} = \left\{ W_h = \left(W_{h_1}, \cdots, W_{h_p}\right) : \begin{array}{rcll} L_{h_i} W_{h_i} &=& f_{h_i}, & \text{in } \Omega^{'}_{i,h_i} \\ W_{h_i} &=& g_{h_i}, & \text{on } \Gamma_{i,h_i}, \end{array} \quad \text{for } i = 1, \cdots, p \right\},$$

and endow $\mathcal{H}$ with the metric

$$\begin{array}{rcl} d\left(U_h, W_h\right) &\equiv& \max_i \left\| U_{h_i} - W_{h_i} \right\|_{\infty, \overline{\Omega}^{'}_{i,h_i}} \\ &=& \max_i \left\| U_{h_i} - W_{h_i} \right\|_{\infty, \partial\Omega^{'}_{i,h_i}} \\ &=& \max_i \left\| U_{h_i} - W_{h_i} \right\|_{\infty, \Gamma^c_{i,h_i}}. \end{array}$$

We note that the second and third definitions of the metric (involving maximum on the boundary $\partial\Omega^{'}_{i,h_i}$ or boundary segment Γ^c_{i,h_i}, respectively) are equivalent to the former by an application of the *discrete maximum principle* since

$$\left\{ \begin{array}{rcll} L_{h_i} U_{h_i} &=& f_{h_i}, & \text{in } \Omega^{'}_{i,h_i} \\ L_{h_i} W_{h_i} &=& f_{h_i}, & \text{in } \Omega^{'}_{i,h_i} \end{array} \right. \implies L_{h_i}\left(U_{h_i} - W_{h_i}\right) = 0, \quad \text{in } \Omega^{'}_{i,h_i},$$

and so by assumption $B1$

$$\begin{array}{rcl} \left\| U_{h_i} - W_{h_i} \right\|_{\infty, \overline{\Omega}^{'}_{i,h_i}} &=& \left\| U_{h_i} - W_{h_i} \right\|_{\infty, \partial\Omega^{'}_{i,h_i}} \\ &=& \left\| U_{h_i} - W_{h_i} \right\|_{\infty, \Gamma^c_{i,h_i}}. \end{array}$$

The latter holds since $U_{h_i} - W_{h_i} = 0$ on Γ_{i,h_i}.

We note that $\mathcal{H}$ is complete under the given metric, since $\mathcal{H}$ is an affine set (defined by linear constraints) in a Euclidean space endowed with the maximum norm. Given $U_h = (U_{h_1}, \cdots, U_{h_p}) \in \mathcal{H}$ we define our mapping $\mathcal{T}U_h = W_h$ as follows

$$\left\{ \begin{array}{rcll} L_{h_i} W_{h_i} &=& f_{h_i}, & \text{on } \Omega^{'}_{i,h_i} \\ W_{h_i} &=& g_{h_i}, & \text{on } \Gamma_{i,h_i} \\ W_{h_i} &=& I^i U_h + z_{h_i}, & \text{on } \Gamma^c_{i,h_i}. \end{array} \right. \tag{10}$$

Clearly $\mathcal{T} : \mathcal{H} \to \mathcal{H}$.

We now verify that $\mathcal{T}$ is a contraction mapping. Accordingly, consider $X_h \in \mathcal{H}$ and $Y_h \in \mathcal{H}$. We estimate $d\left(\mathcal{T}X_h, \mathcal{T}Y_h\right)$. Let $U_h = \mathcal{T}X_h$ and $V_h = \mathcal{T}Y_h$. Using the definition of $\mathcal{T}$ in equation (10) we note that

$$\left\{ \begin{array}{rcll} L_{h_i}\left(U_{h_i} - V_{h_i}\right) &=& 0, & \text{in } \Omega^{'}_{i,h_i} \\ U_{h_i} - V_{h_i} &=& 0, & \text{on } \Gamma_{i,h_i} \\ U_{h_i} - V_{h_i} &=& I^i\left(X_h - Y_h\right), & \text{in } \Gamma^c_{i,h_i}. \end{array} \right.$$

Consequently, we obtain

$$\begin{aligned}
\|U_{h_i} - V_{h_i}\|_{\infty,\Gamma^c_{i,h_i}} &= \|I^i(X_h - Y_h)\|_{\infty,\Gamma^c_{i,h_i}} \\
&\leq \sigma \|X_h - Y_h\|_{\infty,\cup_{j\neq i}\overline{\Omega}_{j,h_j}} \\
&\leq \sigma \max_{j\neq i} \|X_h - Y_h\|_{\infty,\overline{\Omega}_{j,h_j}} \\
&\leq \sigma \max_{j\neq i} \rho_j \|X_h - Y_h\|_{\infty,\partial\Omega'_{j,h_j}} \\
&\leq \delta_0 \max_{j\neq i} \|X_h - Y_h\|_{\infty,\partial\Omega'_{j,h_j}} \\
&\leq \delta_0\, d\,(X_h, Y_h)\,,
\end{aligned}$$

where the fourth line follows by an application of assumption $A2$ on the contraction of homogeneous solutions. Taking maxima over all i on the left-hand side, we obtain

$$\begin{aligned}
d\,(U_h, V_h) &= \max_i \|U_{h_i} - V_{h_i}\|_{\infty,\Gamma^c_{i,h_i}} \\
&\leq \delta_0\, d\,(X_h, Y_h)\,.
\end{aligned}$$

Since $U_h = \mathcal{T}X_h$ and $V_h = \mathcal{T}Y_h$, and since $\delta_0 < 1$ by assumption $A3$, this verifies that $\mathcal{T}$ satisfies a contraction property with contraction factor $\delta_0 < 1$.

Next, we verify that U_h is a fixed point of this contraction mapping. Using the definition of $\mathcal{T}$ in equation (10), we note that if U_h is a fixed point of $\mathcal{T}$ then U_h satisfies

$$\left\{\begin{array}{rcll}
L_{h_i}U_{h_i} &=& f_{h_i}, & \text{on } \Omega'_{i,h_i} \\
U_{h_i} &=& g_{h_i}, & \text{on } \Gamma_{i,h_i} \\
U_{h_i} &=& I^i U_h + z_{h_i}, & \text{on } \Gamma^c_{i,h_i}.
\end{array}\right.$$

Thus, the solution U_h of system (9) is a fixed point of $\mathcal{T}$.

As a final step in establishing the stability of the discrete system (9), we need to determine the distance $d\,(U^0, \mathcal{T}U^0)$ for a suitable choice of initial iterate $U^0 \in \mathcal{H}$. We choose $U^0 = (U^0_{h_1}, \cdots, U^0_{h_p})$ as follows

$$\left\{\begin{array}{rcll}
L_{h_i}U^0_{h_i} &=& f_{h_i}, & \text{on } \Omega'_{i,h_i} \\
U^0_{h_i} &=& g_{h_i}, & \text{on } \Gamma_{i,h_i} \\
U^0_{h_i} &=& z_{h_i}, & \text{on } \Gamma^c_{i,h_i}.
\end{array}\right.$$

Then, $\mathcal{T}U^0$ satisfies

$$\left\{\begin{array}{rcll}
L_{h_i}(\mathcal{T}U^0)_{h_i} &=& f_{h_i}, & \text{on } \Omega'_{i,h_i} \\
(\mathcal{T}U^0)_{h_i} &=& g_{h_i}, & \text{on } \Gamma_{i,h_i} \\
(\mathcal{T}U^0)_{h_i} - I^i U^0 &=& z_{h_i}, & \text{on } \Gamma^c_{i,h_i}.
\end{array}\right.$$

Thus, $U^0_{h_i} - (\mathcal{T}U^0)_{h_i}$ satisfies

$$\left\{\begin{array}{rcll}
L_{h_i}(U^0 - \mathcal{T}U^0)_{h_i} &=& 0, & \text{on } \Omega'_{i,h_i} \\
(U^0 - \mathcal{T}U^0)_{h_i} &=& 0, & \text{on } \Gamma_{i,h_i} \\
(U^0 - \mathcal{T}U^0)_{h_i} &=& I^i U^0, & \text{on } \Gamma^c_{i,h_i}.
\end{array}\right.$$

Using the discrete maximum principle we obtain that

$$\begin{aligned}\left\|(U^0-\mathcal{T}U^0)_{h_i}\right\|_{\infty,\overline{\Omega}'_{i,h_i}} &\leq \|I^iU^0\|_{\infty,\Gamma^c_{i,h_i}}\\ &\leq \sigma\|U^0\|_{\infty,\Omega_h}\\ &\leq \sigma\left(\sum_{i=1}^{p}K_i\|f_{h_i}\|_{\infty,\Omega'_{i,h_i}}+\max\{\|g_{h_i}\|_{\infty,\Gamma_{i,h_i}},\|z_{h_i}\|_{\infty,\Gamma^c_{i,h_i}}\}\right).\end{aligned}$$

Thus

$$d\left(U^0,\mathcal{T}U^0\right)\leq\sigma\left(\sum_{i=1}^{p}K_i\|f_{h_i}\|_{\infty,\Omega'_{i,h_i}}+\max\{\|g_{h_i}\|_{\infty,\Gamma_{i,h_i}},\|z_{h_i}\|_{\infty,\Gamma^c_{i,h_i}}\}\right),$$

and so

$$d\left(U^0,U_h\right)\leq\frac{\sigma}{1-\delta_0}\left(\sum_{i=1}^{p}K_i\|f_{h_i}\|_{\infty,\Omega'_{i,h_i}}+\max\{\|g_{h_i}\|_{\infty,\Gamma_{i,h_i}},\|z_{h_i}\|_{\infty,\Gamma^c_{i,h_i}}\}\right),$$

and using the definition of $d(\cdot,\cdot)$, we obtain that

$$\sum_{i=1}^{p}\|U_{h_i}\|_{\infty,\Omega'_{i,h_i}}\leq\left(1+\frac{\sigma}{1-\delta_0}\right)\left(\sum_{i=1}^{p}K_i\|f_{h_i}\|_{\infty,\Omega'_{i,h_i}}+\max\{\|g_{h_i}\|_{\infty,\Gamma_{i,h_i}},\|z_{h_i}\|_{\infty,\Gamma^c_{i,h_i}}\}\right).$$

This establishes the global stability of scheme (9). □

4. Accuracy of the global discretization. In this section, we estimate the accuracy of the global discretization (7). We assume that the solution $u(x)$ of the original elliptic problem (1) is sufficiently smooth. We have the following theorem.

THEOREM 4.1. *Let $u_h(x)$ denote the restriction of the exact solution $u(x)$ of problem (1) to the composite grid. Let U_h denote the discrete solution. If assumptions B1, B2, B3 hold, and if assumptions A1, A2 and A3 hold, then the error $u_{h_i}-U_{h_i}$ in the discrete solution satisfies the following bounds*

$$\sum_{i=1}^{p}\|u_{h_i}-U_{h_i}\|_{\infty,\Omega'_{i,h_i}}\leq C\left(1+\frac{\sigma}{1-\delta_0}\right)\left(\sum_{i=1}^{p}K_ih_i^{p_i}\|u\|_{p_i+2,\infty,\Omega'_i}+\sum_{i=1}^{p}h_i^{q_i}\|u\|_{q_i,\infty,\Omega_{\Gamma_i^c}}\right).$$

where C, σ, K_i and δ_0 are independent of h_i.

Proof. We substitute u_h into the global discretization to obtain

$$\left\{\begin{array}{rcll}L_{h_i}u_{h_i} &=& f_{h_i}+\alpha_i, & \text{on } \Omega'_{i,h_i}\\ u_{h_i} &=& g_{h_i}, & \text{on } \Gamma_{i,h_i}\\ u_{h_i} &=& I^iu_h+\beta_i, & \text{on } \Gamma^c_{i,h_i},\end{array}\right.$$

where α_i are the local truncation errors and β_i are the local interpolation errors. We define the error e_h by subtracting the exact solution $u_h=(u_{h_1},\cdots,u_{h_p})$ from the discrete solution $U_h=(U_{h_1},\cdots,U_{h_p})$, with $e_{h_i}\equiv u_{h_i}-U_{h_i}$. By subtracting the above equations from the global discretization (7) we obtain

$$\left\{\begin{array}{rcll}L_{h_i}e_{h_i} &=& \alpha_i, & \text{on } \Omega'_{i,h_i}\\ e_{h_i} &=& 0, & \text{on } \Gamma_{i,h_i}\\ e_{h_i}-I^ie_h &=& \beta_i, & \text{on } \Gamma^c_{i,h_i}.\end{array}\right.$$

By applying the stability of the global scheme from Section 3 we obtain that

$$\begin{aligned}\sum_{i=1}^{p}\|e_{h_i}\|_{\infty,\Omega'_{i,h_i}} &\leq \left(1+\frac{\sigma}{1-\delta_0}\right)\left(\textstyle\sum_{i=1}^{p} K_i\|\alpha_i\|_{\infty,\Omega'_{i,h_i}} + \sum_{i=1}^{p}\|\beta_i\|_{\infty,\Gamma^c_{i,h_i}}\right)\\ &\leq C\left(1+\frac{\sigma}{1-\delta_0}\right)\left(\sum_{i=1}^{p} K_i h_i^{p_i}\|u\|_{p_i+2,\infty,\Omega'_i} + \sum_{i=1}^{p} h_i^{q_i}\|u\|_{q_i,\infty,\Omega_{\Gamma^c_i}}\right).\end{aligned}$$

This establishes the accuracy of the global scheme. □

REMARK 4.1. *The parameters C, σ and δ_0 are independent of the ratios h_i/h_j of the mesh sizes.*

REMARK 4.2. *We may alternatively use the largest of the maximum norms on the subgrids since*

$$\max_i \|e_{h_i}\|_{\infty,\Omega'_{i,h_i}} \leq \sum_{i=1}^{p}\|e_{h_i}\|_{\infty,\Omega'_{i,h_i}}.$$

REMARK 4.3. *The above global error bound provides some guidance on the choice of local grid sizes on each subregion and on the accuracy of the local interpolation maps.*

Local grid size. Given a desired global accuracy ϵ, the local grid size h_i on Ω'_i should ideally be chosen to depend on the local smoothness of the solution so that: $h_i^{p_i}\|u\|_{p_i+2,\infty,\Omega'_i} = O(\epsilon/p)$. Thus, a smaller choice for h_i should be used on subregions Ω'_i where the exact solution u is less smooth; i.e., where $\|u\|_{p_i+2,\infty,\Omega'_i}$ is large.

Local interpolation error. The order of accuracy q_i of the local interpolation maps should ideally be chosen depending on the local smoothness of the solution u on the subregion $\Omega_{\Gamma^c_i}$ (which encloses $\Gamma^c_i = \partial\Omega'_i \cap \Omega$) so that: $h_i^{q_i}\|u\|_{p_i,\infty,\Omega_{\Gamma^c_i}} = O(\epsilon/p)$. Alternatively, Ω'_i may be chosen so that its boundary $\partial\Omega'_i$ lies in a region where the exact solution u is smooth; i.e., so that $\|u\|_{p_i,\infty,\Omega_{\Gamma^c_i}}$ is small.

REMARK 4.4. *If $c(x) = 0$ and Ω'_i is a "floating" subdomain, then $\rho_i = 1$ (yielding $\delta_0 \geq 1$). In this case, $\mathcal{T}$ will not be a contraction mapping and the theoretical results in this paper will not apply.*

However, even if $c(x) = 0$ it is possible in some special cases that $\mathcal{T}^n$ can be contractive for some integer $n \geq 2$. To see this, consider the model problem

$$-\frac{d^2u}{dx^2} = f(x), \text{ on } \Omega = (0,3),$$

with $u(0) = u(3) = 0.0$. Choose $\Omega'_1 = (0, 1.5)$, $\Omega'_2 = (0.5, 2.5)$ and $\Omega'_3 = (1.5, 3)$. For this example, Ω'_2 will be a "floating" subdomain with $\rho_2 = 1$. It can be easily verified, since the continuous homogeneous solutions are affine linear in x, that $\rho_1 = \rho_3 = 2/3$. A simple calculation will yeild that $\mathcal{T}^2$ is contractive with contraction factor $2/3$, even though $c(x) = 0$.

More generally, subdomains adjacent to the boundary may have non-trivial contraction factors. If so, the error contraction may "propagate" to interior "floating" domains, as $\mathcal{T}$ is iteratively applied. However, rigorous results are not known to the authors.

5. Iterative methods for solving the global discretization. In this section we discuss two iterative methods for solving the linear system corresponding to the global discretization (7). One is a Schwarz type iterative method and the other is a Krylov subspace iterative method with the additive Schwarz method as a preconditioner.

5.1. A parallel Schwarz iterative method. The iterative procedure we describe is a parallel variant of the Schwarz alternating method, see for instance [6, 10, 13, 14, 22, 27] and involves solving problems on each of the subgrids Ω'_{i,h_i}. We describe the iterative procedure using the contraction mapping $\mathcal{T}$.

For $i = 1, \cdots, p$ compute $U^0_{h_i}$ as follows:

$$\left\{ \begin{array}{rcll} L_{h_i} U^0_{h_i} & = & f_{h_i}, & \text{on } \Omega'_{i,h_i} \\ U^0_{h_i} & = & g_{h_i}, & \text{on } \Gamma_{i,h_i} \\ U^0_{h_i} & = & 0, & \text{on } \Gamma^c_{i,h_i}. \end{array} \right.$$

Until convergence, for $\{n = 0, 1, \cdots\}$ **do:**

Compute $U^{n+1}_h = \mathcal{T} U^n_h$, for $i = 1, \cdots, p$ in *parallel*, as follows:

$$\left\{ \begin{array}{rcll} L_{h_i} U^{n+1}_{h_i} & = & f_{h_i}, & \text{on } \Omega'_{i,h_i} \\ U^{n+1}_{h_i} & = & g_{h_i}, & \text{on } \Gamma_{i,h_i} \\ U^{n+1}_{h_i} & = & I^i U^n_h, & \text{on } \Gamma^c_{i,h_i}. \end{array} \right.$$

Define $U^{n+1}_h = (U^{n+1}_{h_1}, \cdots, U^{n+1}_{h_p})$.

End do

The following theorem provides an estimate for the rate of convergence of U^n_h to the exact discrete solution U_h.

THEOREM 5.1. *Let δ_0 be the contraction factor of $\mathcal{T}$. Then, the iterates $\{U^n_h\}$ converge geometrically to the exact discrete solution U_h, i.e.,*

$$\begin{array}{rcl} d\left(U^{n+1}_h, U_h\right) & \leq & \delta_0 d\left(U^n_h, U_h\right) \\ & \leq & \delta^n_0 d\left(U^0_h, U_h\right). \end{array}$$

Proof. This is a standard result about contraction mappings, see for instance [3]. □

5.2. An additive Schwarz preconditioned GMRES method. The Schwarz iterative method introduced in the previous subsection does converge, but is generally slow when the overlap is small, as one can see from the examples in Section 6.1 of this paper. It turns out a slight modification of the algorithm in Section 5.1 offers a very good preconditioner for any Krylov subspace type iterative methods, such as GMRES [31]. To define the additive Schwarz preconditioner, we let A_i be the stiffness matrix corresponding to the discretization of

$$\left\{ \begin{array}{rcll} L_{h_i} U^0_{h_i} & = & f_{h_i}, & \text{on } \Omega'_{i,h_i} \\ U^0_{h_i} & = & g_{h_i}, & \text{on } \Gamma_{i,h_i} \\ U^0_{h_i} & = & 0, & \text{on } \Gamma^c_{i,h_i}. \end{array} \right.$$

Note that zero Dirichlet boundary condition is used on all subdomain boundaries. We define

$$M^{-1} = diag(A_1^{-1}, A_2^{-1}, \ldots, A_p^{-1})$$

as a block diagonal matrix. Let

$$AU_h = F_h$$

be the matrix form of the global linear system (7). Then the additive Schwarz preconditioned GMRES reads as follows. Find the solution U_h by solving

$$M^{-1}AU_h = M^{-1}F_h$$

using GMRES.

We remark that this is a block diagonal preconditioner, and is fully parallel. In a parallel implementation, if the submeshes and the associated vectors are assigned to different processors, then the preconditioner is communication free. We also note that our maximum principle based theory is not applicable for analyzing the optimal convergence of the additive Schwarz preconditioned GMRES. Numerically, we do observe that when the overlap is fixed, the number of GMRES iterations is independent of the level of refinement. And for a fixed mesh, the number of iterations decreases as we increase the size of the overlap. Several numerical experiments with this method are reported in the next section.

6. Numerical results. In this section, we present some results of sample numerical tests involving non-matching overlapping grids. We refer to [15] for recent literature on matching composite grids, where the interfaces match the grid lines. The elliptic equation we consider is of the form

$$\begin{cases} -\Delta u + cu &= f, \quad \text{in } \Omega, \\ u &= 0, \quad \text{on } \partial\Omega, \end{cases}$$

where c is a constant given below. The domain Ω is the union of some rectangular subdomains. On each of the rectangular subdomains, we use a uniform mesh as indicated in the tables. The local discretization is the standard 5-point finite difference scheme, which satisfies a discrete maximum principle and is stable in the maximum norm.

6.1. Two-subdomain case. We first exam the two subdomain cases. Let $\Omega = [0,2] \times [0,1]$, and we consider a partition involving two subdomains with $\Omega_1 = [0,1] \times [0,1]$, and $\Omega_2 = [1,2] \times [0,1]$. The overlapping domains Ω_1' and Ω_2' are chosen as indicated in the tables. The forcing term f is chosen so that the exact solution is $u(x,y) = (\sin(\pi x) + \sin(\frac{\pi}{2}x))\sin(\pi y)$. For the interpolation maps I^1 and I^2, we use piecewise linear interpolations, and consequently we have

$$\|I^1\|_{\infty,\Gamma_{1,h_1}^c} = 1, \quad \|I^2\|_{\infty,\Gamma_{2,h_2}^c} = 1.$$

TABLE 1

Global error in the maximum norm when varying the level of refinement as $h_1 = 0.2 * 2^{-l}$, $h_2 = 0.25 * 2^{-l}$. *The number of Schwarz iterations is given in* $(\cdot)$. l *is the level of refinement.*

l	$c = 1.0$	$c = 0.1$	$c = 0.01$	$c = 0.0$
0	4.128D-2(11)	4.312D-2(11)	4.331D-2(11)	4.333D-2(11)
1	1.203D-2(11)	1.262D-2(11)	1.269D-2(11)	1.269D-2(11)
2	3.075D-3(11)	3.235D-3(11)	3.252D-3(11)	3.254D-3(11)
3	7.831D-4(11)	8.246D-3(11)	8.290D-3(11)	8.295D-4(11)
4	1.907D-4(11)	2.006D-4(11)	2.017D-4(11)	2.018D-4(11)
5	4.886D-5(11)	5.144D-5(11)	5.172D-5(11)	5.175D-5(11)

The global linear system is solved by the Schwarz alternating method introduced in Section 5, and the stopping criteria for the iteration is to reduce the maximum norm of the initial residual by a factor 10^{-12}.

In our first test, we fix the overlapping parameter to be $\theta = 0.45$. The mesh size in subdomain 1, is chosen to be $h_1 = 0.2 \times 2^{-l}$ and in subdomain 2, it is chosen to be $h_2 = 0.25 \times 2^{-l}$, where l is the level of refinement to be given later. The resulting global grid is non-matching. In Table 1 below, we list the maximum norm of the global errors, and also list in brackets, the number of Schwarz iterations for the values of c listed. As predicted by the theory, since the overlap is fixed, the contraction factor δ_0 is independent of the mesh sizes h_i. It can be easily verified that the global accuracy of the resulting scheme is of 2nd order, and the number of Schwarz iterations is bounded independent of the mesh sizes.

In our second test, we fix the mesh sizes in the subdomains to be $h_1 = 0.2 \times 2^{-5}$ and $h_2 = 0.25 \times 2^{-5}$. The overlapping parameter θ varies as $\theta = 0.45 \times 2^{-5}\gamma$ for some γ to be given in Table 2. Note that for $\gamma = 32 = 2^5$, we recover the overlap used in our previous tests. We tabulate the maximum norm of the global error for several values of c. The number of Schwarz iterations is given in brackets. We note that as the overlap increases, the global accuracy increases, and the number of Schwarz iterations decreases. It can be shown that the contraction factor δ_0 of the mapping $\mathcal{T}$ increases to 1 as the overlap decreases, see for instance [26]. Thus the results are consistent with the theory.

In both of the tests, we note that the error and the number of iterations do not depend strongly on the parameter c which was assumed to be positive in [26] for obtaining the desired theoretical bounds.

6.2. Many-subdomain case. We next run several tests for the cases of many subdomains. Let $\Omega = (0,1) \times (0,1)$. We choose the forcing term f so that the exact solution is $u(x,y) = \sin(\pi x)\sin(\pi y)$. We first divide Ω into $k \times k$ equal subdomains in the checkerboard form, and each subdomain has its own mesh size $h_{i,j}, i,j = 1,\ldots,k$. The overlapping subdomains are obtained by extending each subdomain outward by *ovlp* layers of size $h_{i,j}$. Bilinear interpolations are used for all the subdomain boundaries.

TABLE 2

Global error in the maximum norm and the number of Schwarz iterations when varying the overlapping size. The mesh sizes are $h_1 = 0.2 \times 2^{-5}$, *and* $h_2 = 0.25 \times 2^{-5}$.

γ	$c = 1.0$	$c = 0.1$	$c = 0.01$	$c = 0.0$
1	1.207D-3(264)	1.250D-3(275)	1.255D-3(277)	1.255D-3(277)
2	7.014D-4(137)	7.241D-4(142)	7.265D-4(143)	7.268D-4(143)
4	2.338D-4(71)	2.419D-4(74)	2.427D-4(74)	2.428D-4(74)
8	1.219D-4(37)	1.249D-4(39)	1.253D-4(39)	1.254D-4(39)
16	3.977D-5(20)	4.142D-5(21)	4.159D-5(21)	4.161D-5(21)
32	4.886D-5(11)	5.144D-5(11)	5.172D-5(11)	5.175D-5(11)

TABLE 3

Error in the maximum norm for the case of $4 = 2 \times 2$ *subdomains. The initial submeshes are of sizes* 6×6, 7×7, 8×8 *and* 9×9. *ovlp denotes overlap size and* n *is the total number of unknowns.*

l	0	1	2	3
ovlp	1	2	4	8
n	294	1044	3924	15204
	$c = 0.0$			
Error	4.312D-2	1.162D-2	2.912D-3	6.699D-4
Order		3.7108	3.9904	4.3469
GMRES	11	12	12	13
	$c = 1.0$			
Error	4.219D-2	1.134D-2	2.849D-3	6.560D-4
Order		3.7205	3.9803	4.3430
GMRES	11	12	12	13

We shall restrict ourselves to the case $c = 0.0$. We solve the preconditioned system with GMRES and we stop the iteration when the initial preconditioned residual is reduced by a factor of 10^{-6}. The subdomain problems are solved exactly with the sparse Gaussian elimination.

Table 3 summarizes the four subdomain case. The initial mesh contains four subgrids of sizes 6×6, 7×7, 8×8 and 9×9 and is refined 3 times. The order of accuracy, Order, is obtained by comparing the error with the error of the previous refinement level, as in row 4 of Table 3. n is the total number of unknowns. *ovlp* denotes the number of elements in the overlapping domain. As the level of refinement increases, we increase *ovlp* so that the physical size of the overlap stays the same. Clearly, the order of accuracy is 2. The number of GMRES iterations is nearly independent of the refinement levels.

For the same 4 subdomain case, we fix the mesh sizes at the refinement level $l = 2$

TABLE 4

With same initial submesh sizes as in Table 3, and two levels of refinement, we vary the overlapping sizes.

ovlp	1	2	3	4	5	6
n	3216	3444	3680	3924	4176	4436
	$c = 0.0$					
Error	1.005D-2	5.729D-3	3.526D-3	2.912D-3	2.080D-3	1.832D-3
GMRES	22	17	14	12	11	10
	$c = 1.0$					
Error	9.738D-3	5.558D-3	3.433D-3	2.849D-3	2.042D-3	1.803D-3
GMRES	23	17	14	12	11	10

and vary the overlap sizes. The results are given in Table 4. As one can see, better accuracy can be obtained by using larger overlap, though this accuracy will not improve beyond the accuracy of the local discretizations and interpolation maps. The number of GMRES iterations decreases as we increase the size of overlap.

We remark that it may be noted that when the local grids match, and the standard interpolation map is used (with zero error), the global discretization is equivalent to the standard discretization on the global matching grid. Consequently, increasing the overlap will not improve the global accuracy for matching grids.

We next consider a case when the solution has a much larger gradient in the center of the domain, i.e., we set the exact solution of the problem to

$$u(x, y) = 100 \sin(2\pi x) \sin(2\pi y) e^{-100((x-0.5)^2+(y-0.5)^2)}.$$

Note that a finer mesh is needed in order to resolve the sharp front of the solution in the center of the domain. We compare the accuracy of the solution with two uniform meshes of sizes 128×128 and 256×256, with two non-matching overlapping meshes with nine subdomains whose mesh sizes are given in Table 5. In the non-matching grid case, we use a finer mesh in the center of the domain. As shown in Table 5, a nine subdomain mesh with a total of 3536 mesh points produces a comparably accurate solution as that of a uniform mesh with 16384 mesh points. A non-matching grid with 13465 points gives a more accurate solution than a uniform mesh with 65536 points. Both methods have better than $2nd$ order convergence for this particular test case.

Finally, we test a case that requires a larger mesh ratio. In particular, we consider the general elliptic equation (1) which has both first and zeroth order terms. We use a special right-hand side function, and as a result, the exact solution is of the form

$$u(x, y) = 100 \sin(2\pi x) \sin(2\pi y) \left(e^{-100((x-0.5)^2+(y-0.5)^2)} + e^{-300((x-0.9)^2+(y-0.1)^2)} \right).$$

The coefficients $\vec{b}(x) = (b_1, b_2)$ and $c(x) = c$ will be given in Table 6. Center differences are used for the first order terms. To resolve this solution, finer meshes are needed in the

TABLE 5

Global error in the maximum norm for the case of $9 = 3 \times 3$ *subdomains and a comparison with two uniform grid cases.* n *is the total number of unknows.*

Mesh	uniform 128×128 mesh	uniform 256×256 mesh	16×16 16×16 16×16 16×16 32×32 16×16 16×16 16×16 16×16	31×31 31×31 31×31 31×31 63×63 31×31 31×31 31×31 31×31
ovlp			1	2
n	16384	65536	3536	13465
	$c = 0.0$			
Error	5.841D-2	1.198D-2	6.142D-2	8.659D-3
Order		4.8756		7.0932
GMRES			15	15
	$c = 1.0$			
Error	2.019D-2	5.018D-3	6.123D-2	8.653D-3
Order		4.0235		7.0762
GMRES			15	15

neighborhood of points $(0.5, 0.5)$ and $(0.9, 0.1)$. Different mesh sizes are required in the subdomains containing these two points due to the difference in the smoothness of the exact solution. In the initial test, we use 9 subdomains with a base mesh size 16×16, a finer mesh 64×64 covering the point $(0.5, 0.5)$, and a much finer mesh 96×96 covering the point $(0.9, 0.1)$. Two cells of overlap is used for each subdomain. The maximum norm error and the number of GMRES iterations are given in Table 6. The overlapping composite mesh is then refined uniformly by a factor of 2. Table 6 shows clearly, the error is reduced by a factor large than 4. The large mesh ratio, $191/31 \approx 6$, does not change the order of the accuracy. The number of iterations also stay nearly the same. We also note that the results for $c = 0$ and $c = 1$ are almost identical, with or without the first order terms in the differential equation.

Acknowledgement: We thank the referees for many excellent suggestions.

REFERENCES

[1] G. ABDOULAEV, Y. ACHDOU, J. HONTAND, Y. KUZNETSOV, O. PIRONNEAU, AND C. PRUD'HOMME, *Non-matching grids for fluids*, in the Tenth International Conference on Domain Decomposition Methods for Partial Differential Equations, J. Mandel, C. Farhat, and X.-C. Cai, eds., AMS, Providence, RI, 1998.

[2] Y. ACHDOU, Y. MADAY, AND O. WIDLUND, *Iterative substructuring preconditioners for mortar element methods in two dimensions,* SIAM J. Numer. Anal., 36 (1999), pp. 551–580.

[3] V. ARNOLD, *Ordinary Differential Equations*, Springer-Verlag, New York, 1992.

[4] F. BEN BELGACEM, *The mortar finite element method with Lagrange multipliers*, Numer. Math., 1998. (to appear)

TABLE 6

Global error in the maximum norm for the case of $9 = 3 \times 3$ *subdomains, and with relatively large mesh size ratio.* n *is the total number of unknows.* b_1*,* b_2 *and* c *are the coefficients of the first and zeroth order terms of the elliptic equation (1).*

Mesh	96×96 16×16 16×16 16×16 64×64 16×16 16×16 16×16 16×16	191×191 31×31 31×31 31×31 127×127 31×31 31×31 31×31 31×31
ovlp	2	4
n	16640	65385
	$b_1 = 0.0$, $b_2 = 0.0$, $c = 0.0$	
Error	5.659D-02	1.036D-02
Order		5.4624
GMRES	21	22
	$b_1 = 0.0$, $b_2 = 0.0$, $c = 1.0$	
Error	5.641D-02	1.037D-02
Order		5.4397
GMRES	21	22
	$b_1 = 1.0$, $b_2 = 1.0$, $c = 0.0$	
Error	5.752E-02	1.039D-02
Order		5.5361
GMRES	24	25
	$b_1 = 1.0$, $b_2 = 1.0$, $c = 1.0$	
Error	5.733D-02	1.038D-02
Order		5.5231
GMRES	24	25

[5] C. Bernardi, Y. Maday, and A. Patera, *A new nonconforming approach to domain decomposition: The mortar element method*, in College de France Seminar, H. Brezis and J. Lions, eds., Pitman, 1990.

[6] J. Bramble, J. Pasciak, J. Wang, and J. Xu, *Convergence estimates for product iterative methods with applications to domain decomposition*, Math. Comp., 57 (1991), pp. 1–21.

[7] X.-C. Cai, M. Dryja, and M. Sarkis, *Overlapping non-matching grid mortar element methods for elliptic problems,* SIAM J. Numer. Anal., 36 (1999), pp. 581–606.

[8] M. Casarin, *Schwarz Preconditioners for Spectral and Mortar Finite Element Methods with Applications to Incompressible Fluids*, PhD thesis, Courant Institute of Mathematical Sciences, 1996.

[9] M. Casarin and O. Widlund, *A hierarchical preconditioner for the mortar finite element method*, ETNA 4 (1996), pp. 75–88.

[10] T. Chan and T. Mathew, *Domain decomposition algorithms*, Acta Numerica (1994), pp. 61–143.

[11] G. Chesshire and W. Henshaw, *Composite overlapping meshes for the solution of partial differential equations*, J. of Comput. Phys., 90 (1990), pp. 1–64.

[12] P. Ciarlet, *Discrete maximum principle for finite-difference operators*, Aequationes Math., 4 (1970), pp. 338–353.

[13] M. Dryja, *An additive Schwarz method for elliptic mortar finite element problems in three dimensions*, in the Ninth International Conference on Domain Decomposition Methods for Partial Differential Equations, P. Bjørstad, M. Espedal, and D. Keyes, eds., Wiley & Sons, 1998.

[14] M. Dryja and O. Widlund, *An additive variant of the Schwarz alternating method for the case of many subregions*, Technical Report 339, also Ultracomputer Note 131, Department of Computer Science, Courant Institute of Mathematical Sciences, 1987.

[15] P. Ferket and A. Reusken, *A finite difference discretization method for elliptic problems on composite grids*, Computing, 56 (1996), pp. 343–369.

[16] M. Garbey, Y. kuznetsov, and Y. Vassilevski, *Parallel Schwarz methods for advection-diffusion equations*, SIAM J. Sci. Comput., 1998. (Submitted)

[17] S. Goossens, X.-C. Cai, and D. Roose, *An overlapping non-matching grids method: Some preliminary studies*, in the Tenth International Conference on Domain Decomposition Methods for Partial Differential Equations, J. Mandel, C. Farhat, and X.-C. Cai, eds., AMS, Providence, RI, 1998.

[18] P. Grisvard, *Elliptic Problems in Nonsmooth Domains*, Pitman Publishing, Boston, 1985.

[19] W. Henshaw, *Automatic grid generation*, Acta Numerica, 1996, pp. 121–148.

[20] W. Henshaw, K. Brislawn, D. Brown, G. Chesshire, K. Pao, D. Quinlan, and J. Saltzman, *Overture: An object-oriented framework for solving PDEs on overlapping grids*, LA-UR-97-4033, in Third Symposium on Composite Overset Grid and Solution Technology, Los Alamos, New Mexico, 1996.

[21] Y. Kuznetsov, *Efficient iterative solvers for elliptic finite element problems on non-matching grids*, Russian J. Numer. Anal. Math. Modeling, 10 (1995), pp. 187–211.

[22] P. Lions, *On the Schwarz alternating method I.*, in the First International Symposium on Domain Decomposition Methods for Partial Differential Equations, R. Glowinski, G. Golub, G. Meurant, and J. Périaux, eds., SIAM, Philadelphia, PA, 1988.

[23] P. Lions, *On the Schwarz alternating method. II.*, in the Second International Symposium on Domain Decomposition Methods for Partial Differential Equations, T. Chan, R. Glowinski, J. Périaux, and O. Widlund, eds., SIAM, Philadelphia, PA, 1989.

[24] Y. Maday and A. Patera, *Nonconforming mortar element methods: Application to spectral discretizations*, in the Second International Conference on Decomposition Methods for Partial Differential Equations, T. Chan, R. Glowinski, J. Periaux, and O. Widlund, eds., SIAM Philadelphia, PA, 1989.

[25] T. Mathew, *Uniform convergence of the Schwarz alternating method for solving singularly perturbed advection diffusion equations*, SIAM J. Numer. Anal., 35 (1998), pp. 1663-1683.

[26] T. Mathew and G. Russo, *Stability and convergence of discretizations of linear and semilinear*

parabolic equations on non-matching grids in space-time, Preprint, 1998. (to be submitted to Numer. Math.)

[27] B. Smith, P. Bjørstad, and W. Gropp, *Domain Decomposition: Parallel Multilevel Methods for Elliptic Partial Differential Equations*, Cambridge University Press, 1996.

[28] J. Smoller, *Shock Waves and Reaction-Diffusion Equations*, Springer-Verlag, 1983.

[29] G. Starius, *Composite mesh difference methods for elliptic boundary value problems*, Numer. Math., 28 (1977), pp. 243–258.

[30] J. Steger and J. Benek, *On the use of composite grid schemes in computational aerodynamics*, Comp. Meth. Appl. Mech. Engin., 64 (1987), pp. 301-320.

[31] Y. Saad and M. Schultz, *GMRES: A generalized minimum residual algorithm for solving nonsymmetric linear systems*, SIAM J. Sci. Stat. Comput., 7 (1986), pp. 856–869.

[32] G. Strang and G. J. Fix, *An Analysis of the Finte Element Method*, Prentice Hall, 1973.

[33] J. Thomas, *Finite element matching methods*, in the Fifth International Symposium on Domain Decomposition Methods for Partial Differential Equations, D. Keyes, T. Chan, G. Meurant, J. Scroggs, and R. Voigt, eds., SIAM, Philadelphia, PA, 1992.